Evaluating Relative Heat Stress in the Natura 2000 Site Kras Under Different Climate Change Scenarios: A Case Study Utilizing Multiscale Geographically Weighted Regression

Received/
Prejeto:
30 May 2024
Revised/
Popravljeno:
08 July 2024
Accepted/
Sprejeto:
30 June 2024
Published/
Objavljeno/:
30 June 2024

Danijel Davidovič[1]
danijel.davidovic@um.si

Danijel Ivajnšič[1,2]
dani.ivajnsic@um.si

[1]University of Maribor, Faculty of Arts, Department for Geography; Maribor, Slovenia

[2]University of Maribor, Faculty of Natural sciences and Mathematics, Department of Biology; Maribor, Slovenia

Abstract
The study evaluates relative heat stress in the Natura 2000 site Kras under various climate change scenarios using Multiscale Geographically Weighted Regression (MGWR). Optical and thermal satellite imagery and five future air temperature scenarios were utilized to downscale thermal conditions and evaluate relative heat stress. Results indicate significant spatio-temporal variability in LST, with the southeastern region being particularly susceptible to elevated heat stress. Projections show an overall increase in heat stress due to climate change. The study emphasizes the need for spatially explicit analyses and adaptive strategies to mitigate heat stress impacts on ecosystems and human populations.

Keywords
Land surface temperature, MGWR, NDVI, remote sensing, spatial modelling

Izvleček
Ocena relativne toplotne obremenitve Natura 2000 območja Kras pod različnimi scenariji podnebnih sprememb: Primer uporabe geografsko obtežene regresije
V raziskavi ocenjujemo relativno toplotno obremenitev Natura 2000 območja Kras v različnih scenarijih podnebnih sprememb z uporabo geografsko obtežene regresije (MGWR). Oceno smo oblikovali na podlagi optičnih in termičnih satelitskih podob ter petih napovedi potencialne povprečne temperature zraka, pri čemer smo prostorsko ločljivost slednjih izboljšali z metodo MGWR. Rezultati kažejo značilno prostorsko-časovno variabilnost v LST z večjo toplotno obremenitvijo na jugovzhodu. V splošnem projekcije kažejo povečanje toplotne obremenitve zaradi podnebnih sprememb. Raziskava izpostavlja pomen prostorsko eksplicitnih analiz in prilagodljivih strategij za blaženje vplivov toplotnih obremenitev ekosistemov in prebivalstva.

Ključne besede
Daljinsko zaznavanje, MGWR, NDVI, prostorsko modeliranje, temperatura površja

DOI: https://doi.org/10.18690/rg.19.1.4442

1 Introduction

Land surface temperature (LST) represents the radiative temperature of the Earth's surface, measured as infrared radiation (Liang & Wang, 2020; Pouyan idr., 2022). It is the thermal energy of a thin layer between the atmosphere, soil, vegetation, build-up areas and other land cover types (ESA, 2024). Primarily, LST dynamics are influenced by weather conditions, climatic regimes, vegetation characteristics, land cover/land use patterns, albedo and soil moisture content (Liang, 2018; Khan idr., 2021; Li idr., 2021; *GCOS*, 2024). It represents an essential parameter within the Earth's climate and biological systems and serves as a fundamental metric for assessing various processes of energy and water exchange between the land and the atmosphere (Z.-L. Li & Duan, 2018; Pouyan idr., 2022). Because of its extensive applicable value, LST is recognized as one of the 10 essential climate variables in the biosphere (Hollmann idr., 2013).

Even though the relationship is locally specific, LST influences and is influenced by air temperature and climate change (Gallo idr., 2011). The global air temperature has risen by 1.1°C compared to pre-industrial era, and 2023 was the planet's warmest year on record (NOAA, 2024). Moreover, projections indicate more than 50% likelihood of surpassing 1.5°C by 2040. Alarmingly, in a high-emission scenario, global temperatures may increase in average by 3.3 to 5.7°C by 2100 (IPCC, 2023). The risk is particularly pronounced in Europe, where temperatures have risen at double the rate compared to the global average. Presently, Europe registers a temperature increase of approximately 2.3°C (compared to the preindustrial reference period), becoming thus the fastest warming continent on Earth (WMO, 2023).

Although air temperature cannot be equated to LST directly, it can influence LST spatial and temporal variability (Adão idr., 2023). Global warming is generally higher over land compared to oceans, resulting in a significant increase in LST across 80% of all land surfaces (Farr, 2022; IPCC, 2023). The global average LST has been steadily rising since the 1980s, with higher rates of change observed over the regions north of 45° N (J. Liu idr., 2021). Besides climate change, human activity influence LST by changing natural land cover types and increasing built-up areas resulting in urban heat islands characterized by higher surface and air temperatures (Ivajnšič idr., 2014).

The consequences of rising LST are significant and have wide-ranging impacts on ecosystems and societies. General risks encompass threats concerning both the quality and quantity of water as well as food safety (Zhou idr., 2022). Additionally, higher LST (and the corresponding correlated boundary layer air temperature) can negatively impact human thermal comfort leading to various health risks (Ünsal idr., 2023). Heat stress arises when the body fails to adequately regulate its temperature, particularly in high humidity. Additionally, higher air temperatures contribute to the accumulation of harmful air pollutants, exacerbating respiratory problems and further intensifying the health impacts of heat stress (Vargas Zeppetello idr., 2022; NASA, 2023). The negative consequences on human health encompass dehydration, reduced physical performance and productivity, impaired cognitive functions, cardiovascular complications, potential disability, increased mortality rates and adverse effects on mental health (Ebi idr., 2021).

To preserve fundamental ecosystem services, prevent health risks and enhance general climate change resilience, research of current and potential future LST and

air temperature spatial pattern is essential. Remote sensing, utilizing thermal infrared (TIR, 8–14 μm) instruments aboard various satellites, serves as a useful method for LST data acquisition. These data can be used for detailed LST and air temperature spatio-temporal analysis, monitoring and modeling (K. Li idr., 2021; Gkolemi idr., 2023; Ullah idr., 2023), especially in cloudless, calm weather conditions. However, challenges persist in retrieving and utilizing remotely sensed LST, due to atmospheric interference, limited pixel resolution and the need for specialized knowledge and algorithms for accurate data processing and interpretation (Shiff idr., 2021; Bird idr., 2022; Ahmed idr., 2023). Despite this limitations diverse applications emerged encompassing agriculture (Awais idr., 2022; Garcia-Santos idr., 2022), urban planning (Almeida idr., 2021; Kim & Brown, 2021; Ismaila idr., 2022), climate studies (Tomlinson idr., 2011; Žiberna idr., 2021; Reiners idr., 2023) and environmental research (Blum idr., 2015; Davidovič & Ivajnšič, 2020; Kamal idr., 2022).

To process and extrude useful spatial information from remotely sensed LST data, multiscale geographically weighted regression (MGWR) can be used. The method can be defined as an advanced spatial regression analysis technique that explores geographically varying relationships between dependent variables and predictors resulting in multiple local linear models (Fotheringham idr., 2024). Unlike geographically weighted regression (GWR), MGWR allows for more accurate modeling because of the varying neighborhood (scale) for each predictor (T. Oshan idr., 2019; Comber idr., 2023). The method is relatively new (Fotheringham idr., 2017) but it was already applied in diverse environmental and social research areas including climate studies (Ünsal idr., 2023), habitat quality (Y. Liu idr., 2023), ecosystem services (Sun idr., 2020), house pricing (Zhang idr., 2021), obesity determinants (T. M. Oshan idr., 2020), Lyme disease (Donša idr., 2021) and COVID-19 incidence (Maiti idr., 2021).

Because of its vulnerability to climate change (Ivajnšič & Donša, 2018), we decided to apply and test the MGWR methodology for evaluating relative heat stress in the Natura 2000 site Kras. The region Kras is a limestone plateau in southwestern Slovenia (Figure 1), covering approximately 440 km^2, spanning from northwest to southeast in the Dinaric direction. Because of its porous rock composition, Kras lacks surface water but owing to relatively high precipitation historically enabled deciduous forest formation. However, significant landscape transformation occurred during the Roman era, marked by extensive deforestation resulting in the formation of a dry rocky landscape. Over the past two centuries, Kras has undergone notable transformations again, initially with planned afforestation by black pine, followed by spontaneous afforestation and overgrowth, a trend expected to persist and, in some parts, even increase in the future (Kaligarič & Ivajnšič, 2014; Davidovič idr., 2022).

However, Kras is located in the region where a transition from a continental to a sub-mediterranean climate is evident, thus making it the sunniest area in Slovenia (Zakšek idr., 2007). Due to its permeable rocks and high irradiance, water deficits occur during summer months, when these adverse effects manifest in droughts and wildfires (Veble & Brečko Grubar, 2016). The effect is exacerbated by proliferation of typical vegetation of the intermediate grassland succession stage, dominated by grassland, tall herbs and shrub speciaes, making it more susceptible to fire (Dolgan-Petrič, 1989). Consequently, in 2022, Kras experienced the largest wildfire in Slovenian history, consuming 3,700 hectares over 17 days and causing €26.88 million in damages. In addition to natural factors, the fire's impact was compounded by difficult terrain, hindering firefighter access, and over 10 tons of unexploded

explosives from World War I (STA, 2023). To recover, ongoing reforestation efforts include drought-resistant native deciduous species such as downy oak (*Quercus pubescens*), evergreen oak (*Quercus ilex*) and sessile oak (*Quercus petraea*) (RTVSLO, 2022).

Based on the above mentioned facts, the study addresses the following research questions: (1) can the spatial LST pattern in the study area be modelled with MGWR fitted with normalized vegetation index (NDVI) and average daily air temperature (TAS) values as predictor variables, (2) can the relative change in LST values be predicted for future climate change scenarios, and finally (3) what is the extent of human exposure to increased heat stress in the Natura 2000 site Kras?

2 Methodology

2.1 Data and preprocessing

To model relative heat stress, we employed land surface temperature (LST) as the dependent variable, with mean daily air temperature at 2 meters (TAS) and normalized difference vegetation index (NDVI) as independent variables (predictors). LST values (°C) were derived using the TerrSet module Landsat (TerrSet, 2020) from Landsat 4-5 TM data (thermal band B6) for the summer months (June, July, August) of 1990, 2000, and 2010. Thermal band preprocessing involved conversion from spectral radiance to temperature (Convert to at-satellite brightness temperature). Recent LST values were obtained by averaging summer values across the selected years. Data with a 30-meter pixel resolution for LST calculations were sourced from the EarthExplorer portal (USGS, 2024) managed by the US Geological Survey (USGS).

In the following methodological step, we compiled TAS data for both recent and future periods. Recent values (TAS_rec) were derived by calculating the annual average from monthly values spanning from 1981 to 2010. Future values encompassed the near-term period 2011-2040 (TAS25), mid-term period 2041-2070 (TAS55) and long-term period 2071-2100 (TAS85). Five climate models (GFDL-ESM4, IPSL-CM6A-LR, MPI-ESM1-2-HR, MRI-ESM2-0, UKESM1-0-LL) were employed. For each model two Shared Socioeconomic Pathways (SSP) were considered, an optimistic (ssp126) and a pessimistic (ssp585). The average TAS value across scenarios and time windows was calculated. All climatic data, obtained at approximately 1 km² resolution (30 arc seconds horizontal resolution), were sourced from the CHELSA portal (CHELSA, 2024), managed by the Swiss Federal Institute for Forest, Snow and Landscape Research (WSL).

We used the NDVI as the second predictor. Recent NDVI values (NDVI_rec) were determined using the QGIS Semi-Automatic Classification Plugin (Congedo, 2021) for downloading data as well as atmospheric and radiometric corrections (Convert to reflectance, Dark object subtraction). Landsat 8 data, comprising the red band (B4) and near-infrared band (B5), was utilized for the summer months (June, July, August) of 2010. Subsequent NDVI projections for the near-term period 2011-2040 (NDVI25), mid-term period 2041-2070 (NDVI55) and long-term period 2071-2100 (NDVI85) were derived through a pixel level regression approach, integrating time-NDVI and TAS-NDVI datasets (Davidovič idr., 2022). Data with a 30-meter pixel resolution for NDVI calculations were also sourced from the EarthExplorer portal (USGS, 2024).

Next, 1000 random points were generated across the study area in the QGIS environment. For each point, the following attributes were assigned: x and y coordinates, LST, TAS_rec, TAS25_126, TAS25_585, TAS55_126, TAS55_585, TAS85_126, TAS85_585, NDVI_rec, NDVI25, NDVI55 and NDVI85.

To assess the effect of potential increase or decrease of heat stress on demographics, we employed a 100 x 100 m grid dataset encompassing population data, including age distribution. Data were sourced in vector format from the STAGE portal (STAGE, 2024), which is managed by the Statistical Office of the Republic of Slovenia (SURS).

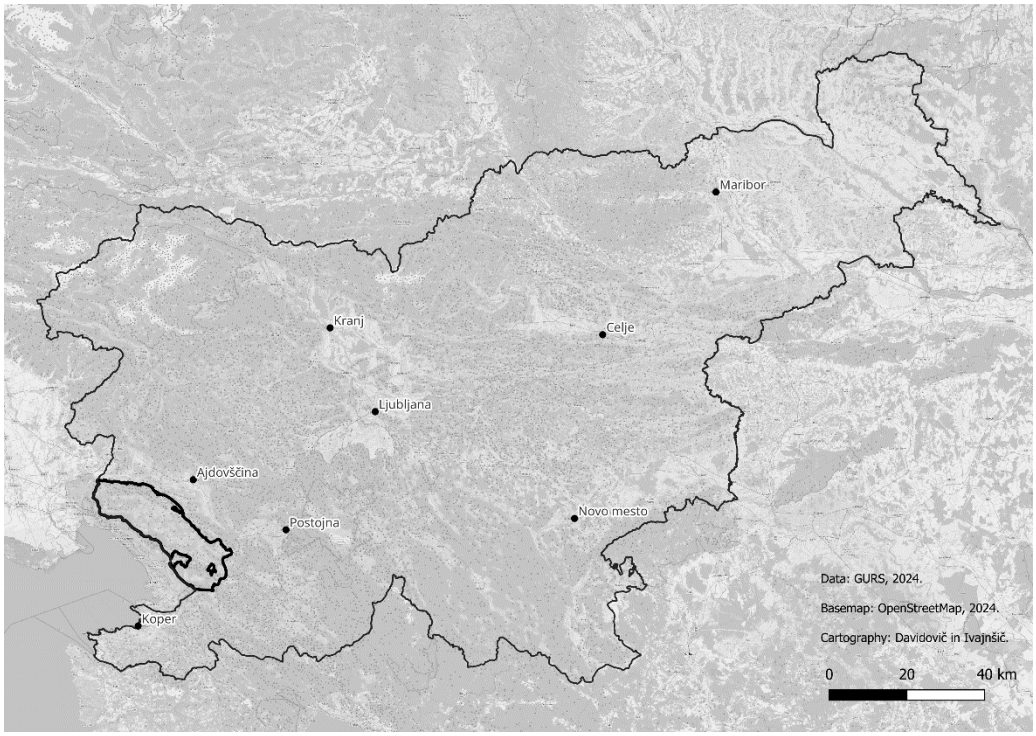

Figure 1: Location of the Natura 2000 site Kras.
Source: Authors.

2.2 Multiscale Geographically Weighted Regression

In conducting regression analysis, we employed MGWR 2.2 (T. Oshan idr., 2019), obtained from the School of Geographical Sciences & Urban Planning website (Arizona State University, 2024). The software processed tabular input of dependent variables and predictors, in our case derived from an attribute table containing 1000 random points. Key settings were: GWR mode (MGWR), spatial kernel (Adaptive, Bisquare), bandwidth searching (Golden selection), variable standardization (Off), initialization (GWR estimates), Monte Carlo test (On), bandwidths confidence (On), SOC (SOC-f), convergence threshold (1e-5), local collinearity (On), model type (Gaussian) and optimization criterion (AICc). Output includes a table presenting local linear equation values and statistical parameters for each point, alongside a text file containing summary statistics for the global and local regression model.

The MGWR analysis provided local coefficients, enabling the calculation of future LST values for each random point. These values were derived for future periods by utilizing the following multiple linear regression equation:

$$LSTx = ß_0 + (NDVIx * ß_{NDVI}) + (TASx\_y * ß_{TAS})$$

where LSTx is the recent or future land surface temperature at a given location, $ß_0$ is the intercept (value of LSTx when NDVI and TAS are 0), NDVIx is the recent or future vegetation index value, $ß_{NDVI}$ is the regression coefficient for NDVI, TASx_y is the recent or future air temperature value in particular scenario and $ß_{TAS}$ is the regression coefficient for TAS. In addition, the standardized residuals (LSTx - LST) were tested for spatial autocorrelation with Moran's I statistics in the R statistical environment (R, 2024) by using the *spdep* package (Bivand, 2022). Model performance was evaluated by comparing global and MGWR regression R^2 and adjusted R^2 values, as well as AIC, AICc and BIC vales. Finally, we calculated relative differences by dividing predicted LST values by recent/actual LST values.

The LSTx values and their relative differences were imported into QGIS (QGIS, 2024) and subjected to interpolation using the Triangulated Irregular Network (TIN) method, employing cubic interpolation (Clough-Toucher) across the research area. These processes provided raster layers for each considered time window with pixel resolution of 30 m. Final values were classified based on quartiles.

Subsequently, based on the areas exhibiting varying degrees of increasing potential heat stress, we quantified the population potentially exposed to elevated risks of heat stress in future periods.

3 Results

3.1 The recent LST, TAS and NDVI status

Recent LST values in the study area range from a minimum of 19.27°C to a maximum of 29.72°C, with an average of 24°C (Figure 2). Elevated LST values are predominantly observed in the central part around Komno, as well as in the northwestern and southern parts of the research area. These areas are characterized by built-up surfaces (settlements), which absorb and retain more electromagnetic radiation. Higher LST values are also noted in grasslands, vineyards, and overgrown areas. Conversely, lower LST values are observed at the edge of the plateau, particularly in the southern areas near Lokev and Divača. These areas, including hills Veliki Ognjivec and Veliko Gradišče to the south and Stol and Mali Ovčjak to the north, are characterized by higher altitudes, steeper slopes and forest land cover.

Recent TAS values range from a minimum of 10.05°C to a maximum of 13.93°C, with an average of 11.83°C (Figure 2). Elevated TAS values are predominantly observed in the northwestern parts around Kostanjevica na Krasu and in the west and southwest of town Komen. These areas, especially dry valley Brestoviški dol, are characterized by the lowest altitudes in the research area. Similarly to LST values, lower TAS values are observed at the edge of the plateau, particularly in the southern and northern areas with higher altitudes. In general, there is a distinct air temperature gradient, with warmer air temperatures in the northwest gradually transitioning to cooler air temperatures in the southeastern part. Some localized warm patches are

interspersed within the predominantly cooler areas, suggesting microclimatic variations due to differences in elevation and land cover.

Recent NDVI values range from a minimum of 0.05 to a maximum of 0.84, with an average of 0.64. Elevated NDVI values are observed across the majority of the region suggesting extensive and dense vegetation cover, a characteristic of forested areas. However, some scattered patches exhibit lower NDVI values, primarily corresponding to build-up surfaces, bare soil, rocky outcrops or agricultural areas with sparse crops.

In general, higher LST are found in areas with lower NDVI values. This inverse relationship suggests that areas with sparse vegetation tend to have higher LST due to reduced shading and less evapotranspiration. Conversely, areas with dense vegetation tend to have lower LST values due to the forest cooling effect. TAS shows a less noticeable relationship with NDVI. Areas with high vegetation cover tend to have slightly lower TAS, suggesting that dense vegetation can moderate local climate. However, TAS is more influenced by broader climatic patterns and elevation changes than by vegetation alone, explaining why the relationship is not as evident as with LST. In addition, there is a general relationship where areas with higher LST also show higher TAS, especially in the northwestern area. However, due to the more localized nature of LST, which is impacted by relief and vegetation, and the broader climatic influences on TAS, the relationship can vary. Areas with low LST and low TAS often overlap, suggesting cooler microclimates both at the surface and in the air, likely due to higher altitudes and denser vegetation cover.

Figure 2: Recent a) land surface temperature, b) air temperature and c) NDVI values across the Natura 2000 site Kras.
Source: Authors.

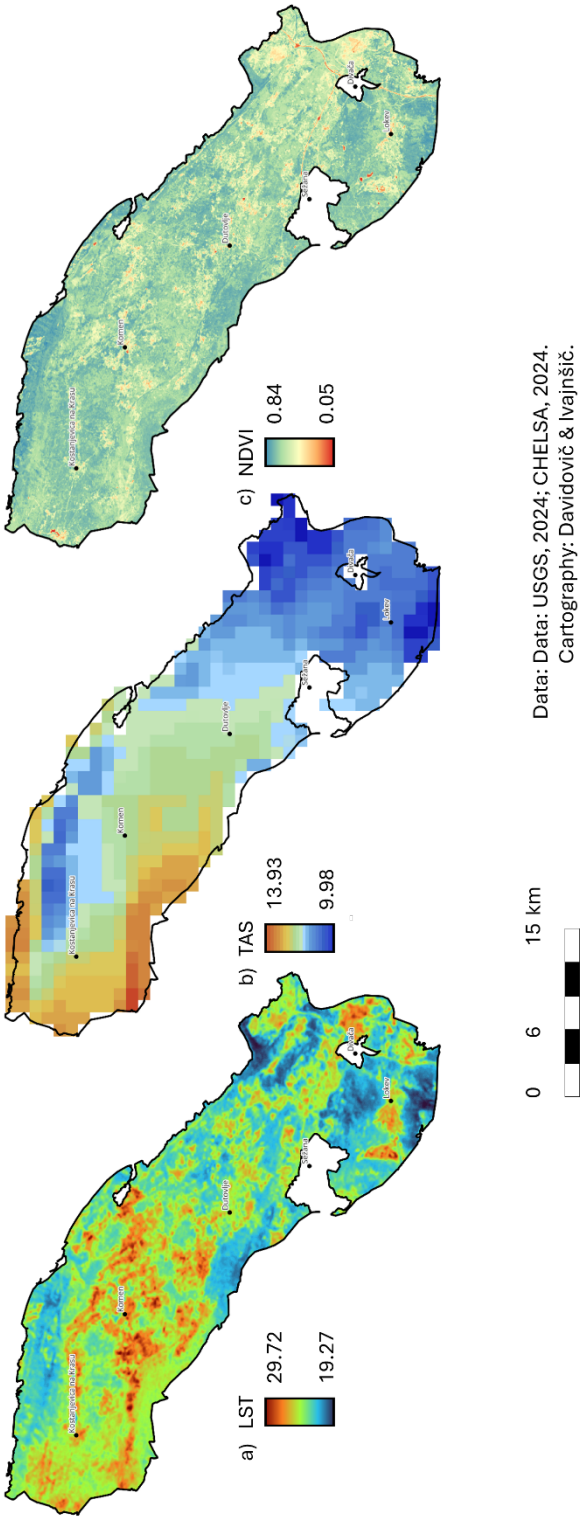
a) LST
29.72
19.27
b) TAS
13.93
9.98
c) NDVI
0.84
0.05
0
6
15 km
Data: Data: USGS, 2024; CHELSA, 2024.
Cartography: Davidovič & Ivajnšič.

3.2 Potential future TAS and NDVI development

Projected TAS values across three future periods range from 11.39°C to 19.37°C depending on different pathways of greenhouse gas emissions and climate change mitigation efforts (Figure 3). In near-term optimistic scenario, TAS values remain relatively low, predominantly between 11°C and approximately 15°C. In near-term pessimistic scenario, TAS values range shows a slight increase compared to the optimistic scenario, with values still mainly below 16°C. The region is characterized by a general warming trend, especially in the northwestern and some central parts. Lower TAS areas persist in higher elevations such as Trstelj and Stol in the north and Veliki Ognjivec and Veliko Gradišče in the southeast. However, their extent is reduced compared to the optimistic scenario.

In mid-term optimistic scenario, TAS values are higher than in near-term period, predominantly ranging from 12°C to about 16°C. The central and southeastern parts remain cooler, while the northwest shows increased warming. The warming trend is evident but remains moderate. In mid-term pessimistic scenario, there is a notable increase in temperature compared to both near-term projections and the mid-term optimistic scenario. Cooler areas are further reduced, with significant warming evident throughout the region, especially in the northwestern part.

In long-term optimistic scenario, TAS values are higher than in previous time sequences, predominantly between 13°C and 17°C. Cooler regions persist in the southeast, but the overall warming trend is recognizable. Lower TAS values dominate in higher elevations, indicating moderate warming compared to the optimistic scenario. In long-term pessimistic scenario, TAS range shifts significantly, with values predominantly between 15°C and 19°C. The entire region transitions to substantially higher values. There are minimal areas with average temperatures below 15°C, highlighting the severe impact of the pessimistic scenario.

In general, there is a clear progressive warming trend from near-term through long-term period across both scenarios. The optimistic scenario depicts a steady warming trend, maintaining lower average air temperatures and preserving cooler areas to some extent. The pessimistic scenario shows a more drastic and accelerated warming trend, with significantly higher average air temperatures and fewer cooler areas. Under the optimistic scenario, the region would experience moderate warming, allowing for adaptation strategies in agriculture, urban planning, and biodiversity conservation. However, under the pessimistic scenario, the region would face severe warming, leading to potential challenges in water availability and increased heat stress with impacts on local ecosystems and human health.

Near-term projections of mean NDVI values at 0.68 indicate extensive dense forest coverage with fewer patches of sparse vegetation, particularly concentrated around built-up areas (Figure 4). Mid-term projections reveal an increase in NDVI mean values to 0.75, signifying enhanced vegetation density throughout the region. The sparse vegetation patches appear to reduce, suggesting forest expansion into previously less vegetated areas. Long-term projections further amplify this trend, with NDVI mean values potentially rising up to 0.84, indicating even more pronounced forest progression. This suggests significant land cover changes and extensification of land use over time. Without management actions, a progressive trend of forest encroachment across the entire region is predicted. This trend could be attributed to various factors, including climate change and land management practices.

DOI: https://doi.org/10.18690/rg.19.1.4445

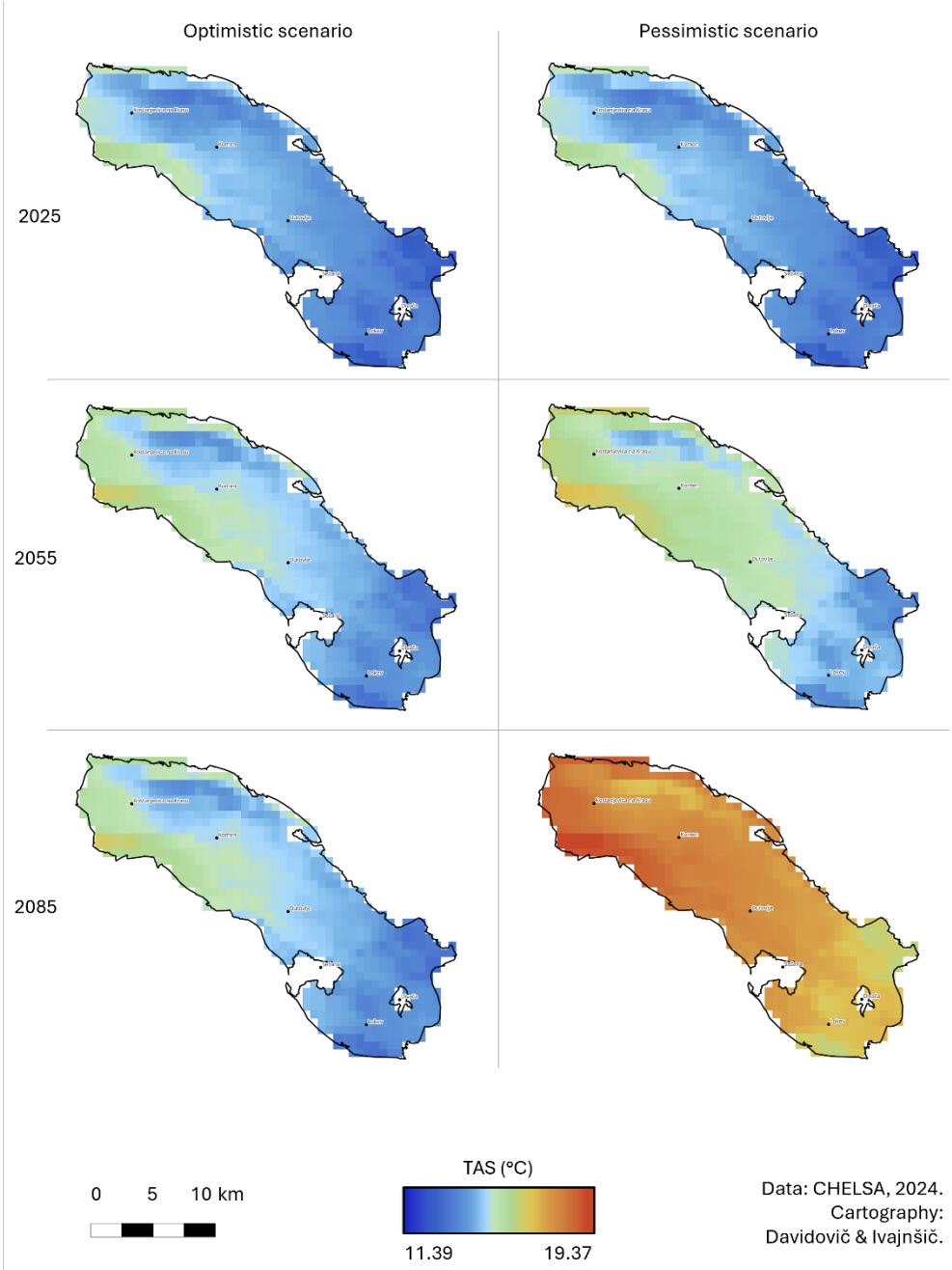

Figure 3: Future air temperature across the Natura 2000 site Kras.
Source: Authors.

Figure 4: Future NDVI values across the Natura 2000 site Kras.
Source: Authors.

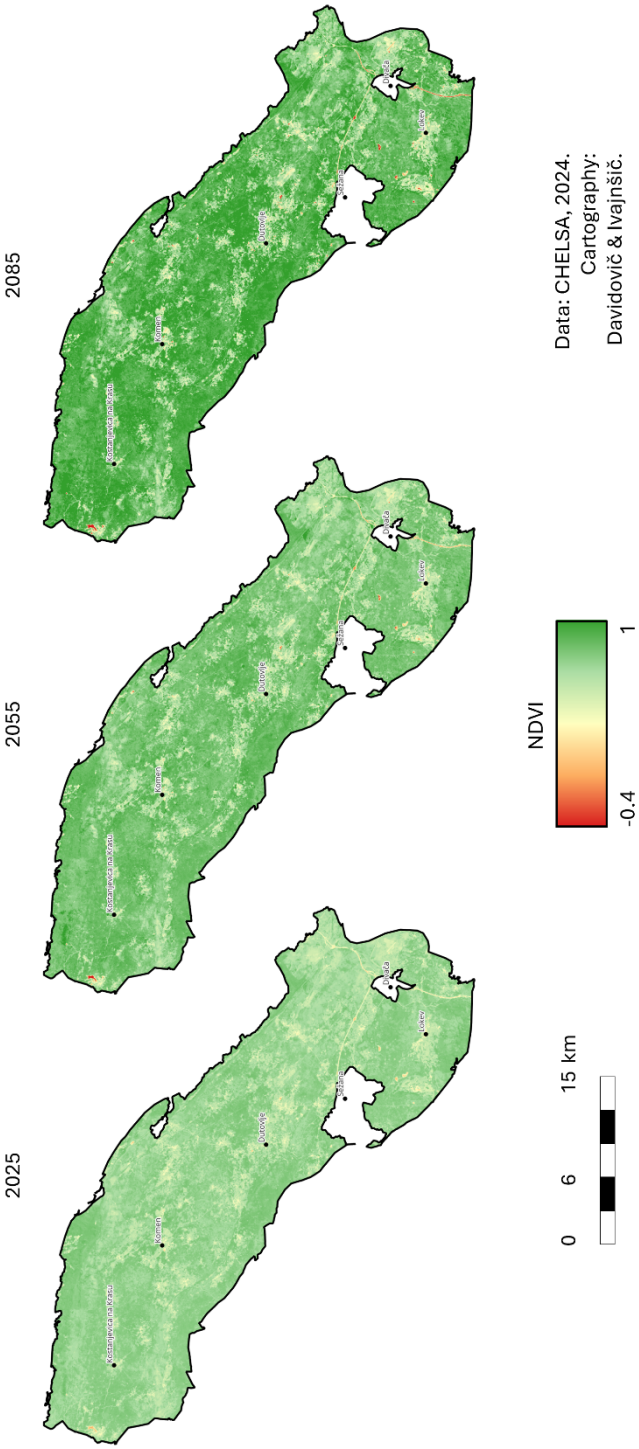

DOI: https://doi.org/10.18690/rg.19.1.4445

3.4 Predicting relative heat stress with Multiscale geographically weighted regression

In the spatial model, LST was employed as the dependent variable, while TAS and NDVI served as predictors. Utilizing the MGWR 2.2 software, global regression results were generated (Table 1) and subsequently compared with the MGWR output (Table 2). From the global regression perspective, both predictors exhibited a statistically significant impact on the dependent variable ($p < \alpha$; $\alpha = 0.05$). TAS demonstrated a positive influence on LST, whereas NDVI exhibited a negative influence on LST. Additionally, the Monte Carlo spatial variability test indicated that both predictors had significant spatially varying estimates, confirming that the effects of these predictors vary across the study area.

Table 1: Global regression results and results of the Monte Carlo test for spatial variability.
Source: Authors.

Residual sum of squares					1358.402
Log-likelihood					-1514.557
AIC					3035.114
AICc					3037.157
R^2					0.482
Adj. R^2					0.481
Variable	**Est.**	**SE**	**t(Est/SE)**	**p-value**	**Spatial variability p-value**
Intercept	16.721	0.683	24.497	0.000	0.000
TAS_rec	1.159	0.055	21.142	0.000	0.000
NDVI_rec	-10.158	0.444	-22.864	0.000	0.000

Table 2: MGWR diagnostic information and summary statistics for MGWR parameter estimates.
Source: Authors.

Residual sum of squares					683.917
Effective number of parameters (trace(S))					95.762
Degree of freedom (n - trace(S))					851.238
Sigma estimate					0.896
Log-likelihood					-1189.628
Degree of Dependency (DoD)					0.495
AIC					2572.781
AICc					2595.059
BIC					3042.397
R^2					0.739
Adj. R^2					0.710
Variable	**Mean**	**STD**	**Min**	**Median**	**Max**
Intercept	23.516	2.005	19.800	23.885	26.146
TAS_rec	0.598	0.116	0.406	0.585	0.836
NDVI_rec	-10.243	0.686	-11.815	-10.273	-8.644

The global regression model exhibited a moderately weak fit (R^2 = 48%). In contrast, the MGWR approach significantly enhanced model performance, evidenced by a 2-

times lower residual sum of squares and a higher percentage of explained variance (R^2 = 74%). Additionally, the AIC and the AICc values were notably lower in the MGWR model, indicating better model performance.

These diagnostics underscore the enhanced explanatory power and fit of the MGWR model relative to the global regression model. The parameter estimates of the MGWR model varied across the study area, effectively capturing local variations in the relationships between the dependent variable and the predictors. This spatial adaptability of the MGWR model provides a more detailed understanding of the factors influencing heat stress.

Moreover, the statistical insignificance (Moran's Index value = 0.06; p>α; α = 0.05) of standardized residual (under- and over-predictions) spatial autocorrelation additionally proved the appropriate MGWR model specification. Thus, MGWR can be used to statistically downscale global climate model-based air temperature variables like TAS for specific research areas.

3.5 Heat stress areas and population

Both near-term scenarios show a slight increase in LST with isolated areas experiencing slight decrease (Figure 6). According to mid-term projection, the optimistic scenario is characterized by expanding areas of decreased LST, especially in the northwest, while the pessimistic scenario shows more areas with slight increase similarly to near-term projections. Long-term optimistic scenario shows a substantial area with slight to moderate decreases in LST, while the pessimistic scenario indicates widespread increases, particularly in the southern part of the region. In general, the whole region is expected to experience a slight increase in LST due to increasing temperature owing to climate change. However, according to the long-term optimistic projection, the majority of the region is expected to record a decrease in LST. Similarly to other research (Hulley idr., 2019; J. Liu idr., 2021) we found that decreased LST aligns with high NDVI values due to denser vegetation typical for encroachment processes.

Despite identifying areas with decreasing LST in the future, significant risks remain for population in areas experiencing slight, moderate or significant increases in LST. In general, Slovenia's population is projected to decline by 7% by 2100, despite anticipated increases in fertility rates. Additionally, life expectancy at birth is expected to rise, leading to an aging population, with individuals aged 65 and older constituting over 32% of the population by 2100 (SURS, 2023). Given that the young and elderly are most susceptible to heat stress (Kenny idr., 2010; UNICEF, 2023), the projected temperature rise is particularly concerning. However, despite practically ignoring the demographic temporal dynamics over the next decades, our assessment nevertheless highlights the increasing vulnerability of these age groups and emphasizes the need for appropriate and timely countermeasures. Some of the areas where the elderly population is concentrated are settlements of Dutovlje, Lokev and Komen (Figure 5).

In a near-term optimistic scenario, 70.6% of individuals, including 9.3% of young individuals and 17.8% of elderly individuals, reside in areas experiencing an increase in LST. Conversely, in the near-term pessimistic scenario, the number of people affected by the potential rise in LST slightly decreases to 70%, encompassing 9.2% of young individuals and 17.7% of elderly individuals. The differences between the two scenarios are subtle. The optimistic scenario predicts a marginally higher total

population (+0.5 percentage points), as well as slightly more young and elderly populations (+0.1 percentage point each) exposed to increased LST compared to the pessimistic scenario.

In a long-term optimistic scenario, 44% of individuals, including 5.8% of young individuals and 11.3% of elderly individuals, reside in areas experiencing a potential increase in LST. In contrast, in a long-term pessimistic scenario, the population affected by rising LST increases significantly to 83.8% of individuals, comprising 11.4% of young individuals and 21.1% of elderly individuals. Thus, in the pessimistic scenario, the overall affected population is nearly doubled compared to the optimistic scenario. Specifically, the number of young individuals affected increases by approximately 97%, while the number of elderly individuals affected shows an increase of about 86%. This indicates that under more adverse conditions, a significantly larger portion of both young and elderly populations are subjected to heightened LST, which could exacerbate the associated health risks and necessitate more robust adaptive measures.

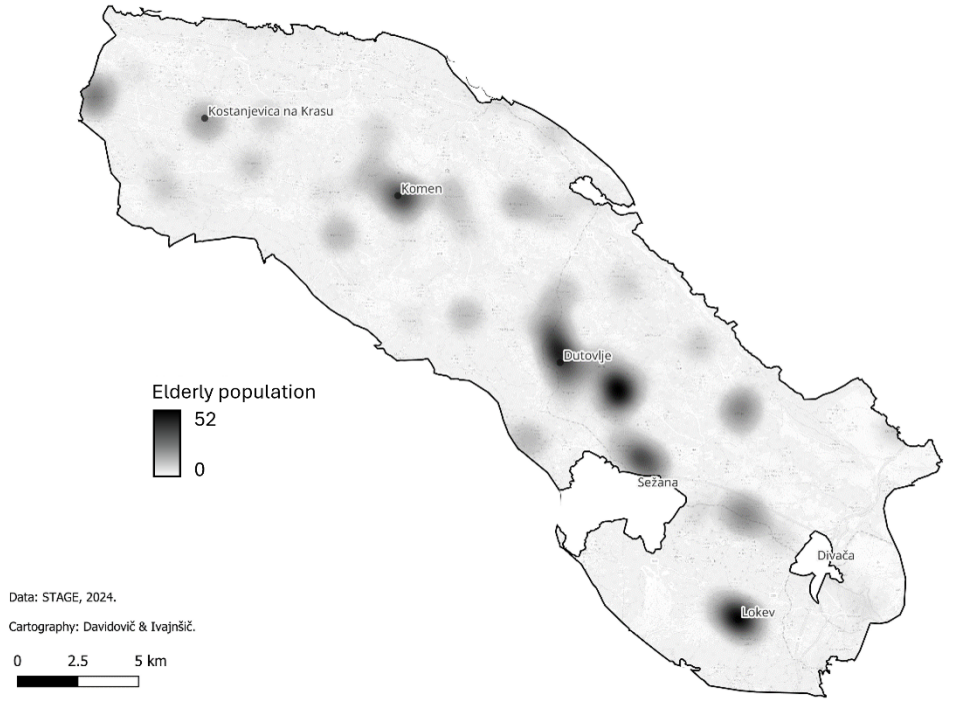

Figure 5: Elderly population across the Natura 2000 site Kras (variable is shown as an interpolated grid for visualization purposes only).
Source: Authors.

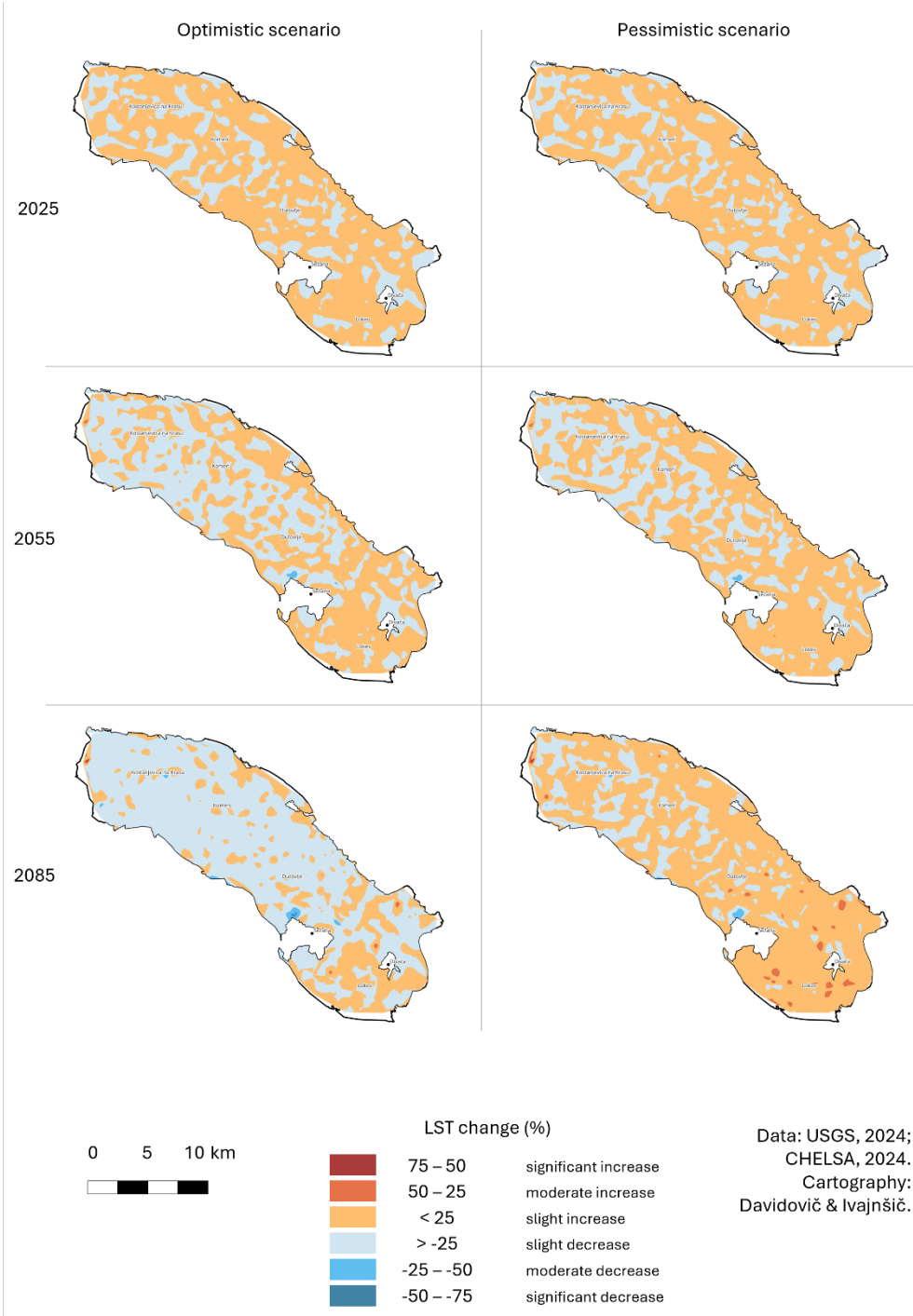

Figure 6: Future potential relative differences in heat stress across the Natura 2000 site Kras.
Source: Authors.

4 Conclusion

LST is a crucial variable for monitoring environmental changes and their impacts on the climate and biosphere at local, regional, and global scales. We used MGWR to model the spatial and temporal variability of LST using NDVI and TAS as predictor variables. Thus, the provided global climate model-based TAS variables (recent and future scenarios [pixel size = 1 km]) were downscaled for our specific study area (Natura 2000 site Kras) and then used to evaluate relative change in heat stress under predicated climate change scenarios in much better spatial resolution (pixel size = 30 m). The findings demonstrate significant spatial variability in LST (and thus potentially TAS), with higher temperatures notably in the southeastern parts of the study area. Future climate change scenarios predict an overall increase in relative heat stress, though areas with dense vegetation may experience a reduction. Human exposure to increased relative heat stress is projected to rise, with vulnerable populations being significantly affected.

Our findings confirm that the MGWR model effectively captures the spatial variability of LST in the study area. The integration of NDVI and TAS as predictors provides a robust framework for understanding the relationship between surface thermal conditions, air temperature and vegetation cover. The MGWR model successfully captured the spatial heterogeneity in LST, demonstrating a pronounced inverse relationship between NDVI and LST. Specifically, areas with higher vegetation cover typically exhibit lower LST, attributed to increased shading and evapotranspiration. Conversely, TAS exhibits a less pronounced relationship with LST, as it is more influenced by broader climatic patterns and elevation changes. However, our study proofs that MGWR can be used to statistically downscale mean air temperature data (TAS) provided by global climate models for better regional and local scale studies.

The study confirms that relative changes in heat stress can be predicted for future climate change scenarios in better spatial resolution. The projections indicate a general increase in heat stress across the study area, with specific variations contingent on the scenario considered. The study delineates future relative heat stress patterns for near-term, mid-term, and long-term periods under both optimistic and pessimistic scenarios. These projections reveal that there is a consistent trend towards higher heat stress values, reflecting the broader impacts of global climate change. The magnitude of heat stress increase varies significantly between the scenarios, with the optimistic scenario projecting more moderate increases in heat stress and the pessimistic scenario suggesting more severe rises. Additionally, the rate of relative heat stress increase is not uniform over time, with near-term projections showing more gradual changes and mid-term to long-term projections indicating more pronounced increases. Spatial heterogeneity is also evident, as areas characterized by dense vegetation may experience smaller increases in heat stress or even slight decreases. These predictions emphasize the need for tailored regional planning and climate adaptation strategies approaches to address the specific thermal stress responses of different areas within the study region.

Human exposure to increased potential heat stress is anticipated to be substantial, particularly among vulnerable populations. The research projects that a significant portion of the population will inhabit areas experiencing elevated LST and heat stress under both optimistic and pessimistic climate scenarios. By the end of the century, the elderly, who are especially susceptible to heat stress, will be disproportionately affected. Beyond the direct impact on human health, elevated heat conditions can

also affect biodiversity, traditional activities such as the production of Karst Prosciutto ham, the spread of vector-borne diseases, the incidence of wildfires, drought, water availability, tourism activities and pollution levels. The research highlights the necessity for developing comprehensive adaptive strategies to mitigate the impacts of heat stress on both ecosystems and human health in the face of global warming.

The application of MGWR in this study has yielded a new understanding of heat stress patterns within the Natura 2000 site Kras under various climate change scenarios. Our findings delineate stark contrasts between optimistic and pessimistic scenarios, underscoring the potential benefits of implementing effective climate policies. The study also highlights the challenges posed by demographic changes in Slovenia, particularly the increasing proportion of elderly individuals, which is expected to place significant demands on healthcare systems. This demographic trend underscores the urgency of developing proactive strategies in healthcare services to ensure optimal living conditions amidst the anticipated impacts of climate change. Comprehensive and forward-thinking approaches are essential to address the compounded effects of climate and demographic changes, ensuring resilience and well-being of ecosystems and society.

References

Adão, F., Fraga, H., Fonseca, A., Malheiro, A. C., & Santos, J. A. (2023). The Relationship between Land Surface Temperature and Air Temperature in the Douro Demarcated Region, Portugal. Remote Sensing, 15(22), Article 22. https://doi.org/10.3390/rs15225373

Ahmed, M. R., Ghaderpour, E., Gupta, A., Dewan, A., & Hassan, Q. K. (2023). Opportunities and Challenges of Spaceborne Sensors in Delineating Land Surface Temperature Trends: A Review. IEEE Sensors Journal, 23(7), 6460–6472. https://doi.org/10.1109/JSEN.2023.3246842

Almeida, C. R. de, Teodoro, A. C., & Gonçalves, A. (2021). Study of the Urban Heat Island (UHI) Using Remote Sensing Data/Techniques: A Systematic Review. Environments, 8(10), Article 10. https://doi.org/10.3390/environments8100105

ARSO. (2019). Climate change projections for Slovenia over the 21st century (p. 23). https://www.meteo.si/uploads/probase/www/climate/text/en/publications/OPS21_brosura_ENG.pdf

Awais, M., Li, W., Hussain, S., Cheema, M. J. M., Li, W., Song, R., & Liu, C. (2022). Comparative Evaluation of Land Surface Temperature Images from Unmanned Aerial Vehicle and Satellite Observation for Agricultural Areas Using In Situ Data. Agriculture, 12(2), Article 2. https://doi.org/10.3390/agriculture12020184

Bird, D. N., Banzhaf, E., Knopp, J., Wu, W., & Jones, L. (2022). Combining Spatial and Temporal Data to Create a Fine-Resolution Daily Urban Air Temperature Product from Remote Sensing Land Surface Temperature (LST) Data. Atmosphere, 13(7), Article 7. https://doi.org/10.3390/atmos13071152

Bivand, R. (2022). R Packages for Analyzing Spatial Data: A Comparative Case Study with Areal Data. Geographical Analysis, 54(3), 488–518. https://doi.org/10.1111/gean.12319

Blum, M., Lensky, I. M., Rempoulakis, P., & Nestel, D. (2015). Modeling insect population fluctuations with satellite land surface temperature. Ecological Modelling, 311, 39–47. https://doi.org/10.1016/j.ecolmodel.2015.05.005

Byrne, M. P., & O'Gorman, P. A. (2018). Trends in continental temperature and humidity directly linked to ocean warming. Proceedings of the National Academy of Sciences of the United States of America, 115(19), 4863–4868. https://doi.org/10.1073/PNAS.1722312115

CHELSA. (2024). Chelsa Climate. https://chelsa-climate.org/downloads/

Comber, A., Brunsdon, C., Charlton, M., Dong, G., Harris, R., Lu, B., Lü, Y., Murakami, D., Nakaya, T., Wang, Y., & Harris, P. (2023). A Route Map for Successful Applications of Geographically Weighted Regression. Geographical Analysis, 55(1), 155–178. https://doi.org/10.1111/gean.12316

Congedo, L. (2021). Semi-Automatic Classification Plugin: A Python tool for the download and processing of remote sensing images in QGIS. Journal of Open Source Software, 6(64), 3172. https://doi.org/10.21105/joss.03172

Davidovič, D., & Ivajnšič, D. (2020). Indeks vlažnosti tal Pomurja. Revija Za Geografijo, 15(1), 91–107.

Davidovič, D., Ivajnsič, D., & Čuš, J. (2022). Interakcija naravnih in družbenih razmer kot pospeševalec zaraščanja Krasa (pp. 101–120). https://doi.org/10.18690/um.fnm.8.2022.5

Dolgan-Petrič, M. (1989). Gozdni požari na kraškem gozdnogospodarskem območju Slovenije. Geografski Vestnik, 61, 71–82.

Donša, D., Grujić, V. J., Pipenbaher, N., & Ivajnšič, D. (2021). The Lyme Borreliosis Spatial Footprint in the 21st Century: A Key Study of Slovenia. International Journal of Environmental Research and Public Health, 18(22), Article 22. https://doi.org/10.3390/ijerph182212061

Ebi, K. L., Capon, A., Berry, P., Broderick, C., Dear, R. de, Havenith, G., Honda, Y., Kovats, R. S., Ma, W., Malik, A., Morris, N. B., Nybo, L., Seneviratne, S. I., Vanos, J., & Jay, O. (2021). Hot weather and heat extremes: Health risks. The Lancet, 398(10301), 698–708. https://doi.org/10.1016/S0140-6736(21)01208-3

ESA. (2024). Land Surface Temperature. https://climate.esa.int/en/projects/land-surface-temperature/

ESRI. (2024). Multiscale Geographically Weighted Regression (MGWR) (Spatial Statistics)—ArcGIS Pro | Documentation. https://pro.arcgis.com/en/pro-app/latest/tool-reference/spatial-statistics/multiscale-geographically-weighted-regression.htm

Farr, D. (2022). Temperature trends in some major countries from the 1980s to 2019. Journal of Geographical Sciences, 32(1), 79–100. https://doi.org/10.1007/s11442-022-1937-1

Fotheringham, A. S., Oshan, T., & Li, Z. (2024). Multiscale geographically weighted regression: Theory and practice (First edition). CRC Press.

Fotheringham, A. S., Yang, W., & Kang, W. (2017). Multiscale Geographically Weighted Regression (MGWR). Annals of the American Association of Geographers, 107(6), 1247–1265. https://doi.org/10.1080/24694452.2017.1352480

Gallo, K., Hale, R., Tarpley, D., & Yu, Y. (2011). Evaluation of the Relationship between Air and Land Surface Temperature under Clear- and Cloudy-Sky Conditions. Journal of Applied Meteorology and Climatology, 50(3), 767–775. https://doi.org/10.1175/2010JAMC2460.1

Garcia-Santos, V., Niclòs, R., & Valor, E. (2022). Evapotranspiration Retrieval Using S-SEBI Model with Landsat-8 Split-Window Land Surface Temperature Products over Two European Agricultural Crops. Remote Sensing, 14(11), Article 11. https://doi.org/10.3390/rs14112723

GCOS. (2024). Land Surface Temperature. https://gcos.wmo.int/en/essential-climate-variables/land-temperature

Gkolemi, M., Mitraka, Z., & Chrysoulakis, N. (2023). Local scale surface temperature estimation by downscaling satellite thermal infrared observations using neural networks. 2023 Joint Urban Remote Sensing Event (JURSE), 1–4. https://doi.org/10.1109/JURSE57346.2023.10144083

Hollmann, R., Merchant, C. J., Saunders, R., Downy, C., Buchwitz, M., Cazenave, A., Chuvieco, E., Defourny, P., Leeuw, G. de, Forsberg, R., Holzer-Popp, T., Paul, F., Sandven, S., Sathyendranath, S., Roozendael, M. van, & Wagner, W. (2013). The ESA Climate Change Initiative: Satellite Data Records for Essential Climate

Variables. Bulletin of the American Meteorological Society, 94(10), 1541–1552. https://doi.org/10.1175/BAMS-D-11-00254.1

Hulley, G. C., Ghent, D., Göttsche, F. M., Guillevic, P. C., Mildrexler, D. J., & Coll, C. (2019). Land Surface Temperature. In Taking the Temperature of the Earth (pp. 57–127). Elsevier. https://doi.org/10.1016/B978-0-12-814458-9.00003-4

IPCC. (2023). Climate Change 2022 – Impacts, Adaptation and Vulnerability: Working Group II Contribution to the Sixth Assessment Report of the Intergovernmental Panel on Climate Change (1st ed.). Cambridge University Press. https://doi.org/10.1017/9781009325844

Ismaila, A.-R. B., Muhammed, I., & Adamu, B. (2022). Modelling land surface temperature in urban areas using spatial regression models. Urban Climate, 44, 101213. https://doi.org/10.1016/j.uclim.2022.101213

Ivajnšič, D., Kaligarič, M., & Žiberna, I. (2014). Geographically weighted regression of the urban heat island of a small city. Applied Geography, 53, 341–353. https://doi.org/10.1016/j.apgeog.2014.07.001

Ivajnšič, D., & Žiberna, I. (2019). The effect of weather patterns on winter small city urban heat islands. Meteorological Applications, 26(2), 195–203. https://doi.org/10.1002/met.1752

Kaligarič, M., & Ivajnšič, D. (2014). Vanishing landscape of the "classic" Karst: Changed landscape identity and projections for the future. Landscape and Urban Planning, 132, 148–158. https://doi.org/10.1016/j.landurbplan.2014.09.004

Kamal, H., Aljeri, M., Abdelhadi, A., Thomas, M., & Dashti, A. (2022). Environmental Assessment of Land Surface Temperature Using Remote Sensing Technology. Environmental Research, Engineering and Management, 78(3), Article 3. https://doi.org/10.5755/j01.erem.78.3.31568

Kenny, G. P., Yardley, J., Brown, C., Sigal, R. J., & Jay, O. (2010). Heat stress in older individuals and patients with common chronic diseases. CMAJ : Canadian Medical Association Journal, 182(10), 1053–1060. https://doi.org/10.1503/cmaj.081050

Kestens, Y., Brand, A., Fournier, M., Goudreau, S., Kosatsky, T., Maloley, M., & Smargiassi, A. (2011). Modelling the variation of land surface temperature as determinant of risk of heat-related health events. International Journal of Health Geographics, 10(1), 7. https://doi.org/10.1186/1476-072X-10-7

Khan, A., Chatterjee, S., & Weng, Y. (2021). 2—Characterizing thermal fields and evaluating UHI effects. In A. Khan, S. Chatterjee, & Y. Weng (Eds.), Urban Heat Island Modeling for Tropical Climates (pp. 37–67). Elsevier. https://doi.org/10.1016/B978-0-12-819669-4.00002-7

Kim, S. W., & Brown, R. D. (2021). Urban heat island (UHI) intensity and magnitude estimations: A systematic literature review. Science of The Total Environment, 779, 146389. https://doi.org/10.1016/j.scitotenv.2021.146389

Li, K., Guan, K., Jiang, C., Wang, S., Peng, B., & Cai, Y. (2021). Evaluation of Four New Land Surface Temperature (LST) Products in the U.S. Corn Belt: ECOSTRESS, GOES-R, Landsat, and Sentinel-3. IEEE Journal of Selected Topics in Applied Earth Observations and Remote Sensing, 14, 9931–9945. https://doi.org/10.1109/JSTARS.2021.3114613

Li, Z.-L., & Duan, S.-B. (2018). Land Surface Temperature. In Comprehensive Remote Sensing (pp. 264–283). Elsevier. https://doi.org/10.1016/B978-0-12-409548-9.10375-6

Li, Z.-L., Wu, H., Duan, S.-B., Zhao, W., Ren, H., Liu, X., Leng, P., Tang, R., Ye, X., Zhu, J., Sun, Y., Si, M., Liu, M., Li, J., Zhang, X., Shang, G., Tang, B.-H., Yan, G., & Zhou, C. (2023). Satellite Remote Sensing of Global Land Surface Temperature: Definition, Methods, Products, and Applications. Reviews of Geophysics, 61(1), e2022RG000777. https://doi.org/10.1029/2022RG000777

Liang, S. (2018). 5.01 - Volume 5 Overview: Recent progress in Remote Sensing of Earth's Energy Budget. In S. Liang (Ed.), Comprehensive Remote Sensing (pp. 1–31). Elsevier. https://doi.org/10.1016/B978-0-12-409548-9.10365-3

Liang, S., & Wang, J. (Eds.). (2020). Chapter 7—Land surface temperature and thermal infrared emissivity. In Advanced Remote Sensing (Second Edition) (pp. 251–295). Academic Press. https://doi.org/10.1016/B978-0-12-815826-5.00007-6

Liu, J., Hagan, D. F. T., & Liu, Y. (2021). Global Land Surface Temperature Change (2003–2017) and Its Relationship with Climate Drivers: AIRS, MODIS, and ERA5-Land Based Analysis. Remote Sensing, 13(1), Article 1. https://doi.org/10.3390/rs13010044

Liu, Y., Wang, Y., Lin, Y., Ma, X., Guo, S., Ouyang, Q., & Sun, C. (2023). Habitat Quality Assessment and Driving Factors Analysis of Guangdong Province, China. Sustainability, 15(15), Article 15. https://doi.org/10.3390/su151511615

Maiti, A., Zhang, Q., Sannigrahi, S., Pramanik, S., Chakraborti, S., Cerda, A., & Pilla, F. (2021). Exploring spatiotemporal effects of the driving factors on COVID-19 incidences in the contiguous United States. Sustainable Cities and Society, 68, 102784. https://doi.org/10.1016/j.scs.2021.102784

NASA. (2023, December 31). [Text.Article]. Vegetation & Land Surface Temperature; NASA Earth Observatory. https://earthobservatory.nasa.gov/global-maps/MOD_NDVI_M/MOD_LSTD_M

NOAA. (2024). Annual 2023 Global Climate Report. https://www.ncei.noaa.gov/access/monitoring/monthly-report/global/202313

Oshan, T., Li, Z., Kang, W., Wolf, L., & Fotheringham, A. (2019). MGWR: A Python Implementation of Multiscale Geographically Weighted Regression for Investigating Process Spatial Heterogeneity and Scale. ISPRS International Journal of Geo-Information, 8(6), 269. https://doi.org/10.3390/ijgi8060269

Oshan, T. M., Smith, J. P., & Fotheringham, A. S. (2020). Targeting the spatial context of obesity determinants via multiscale geographically weighted regression. International Journal of Health Geographics, 19(1), 11. https://doi.org/10.1186/s12942-020-00204-6

Pablos, M., Martínez-Fernández, J., Piles, M., Sánchez, N., Vall-llossera, M., & Camps, A. (2016). Multi-Temporal Evaluation of Soil Moisture and Land Surface Temperature Dynamics Using in Situ and Satellite Observations. Remote Sensing, 8(7), Article 7. https://doi.org/10.3390/rs8070587

Pouyan, S., Rahmanian, S., Amindin, A., & Pourghasemi, H. R. (2022). Chapter 15—Spatial and seasonal modeling of the land surface temperature using random forest. In H. R. Pourghasemi (Ed.), Computers in Earth and Environmental Sciences (pp. 221–234). Elsevier. https://doi.org/10.1016/B978-0-323-89861-4.00035-X

QGIS. (2024, April 19). https://qgis.org/en/site/forusers/download.html

R. (2024). The R Project for Statistical Computing. https://www.r-project.org/

Reiners, P., Sobrino, J., & Kuenzer, C. (2023). Satellite-Derived Land Surface Temperature Dynamics in the Context of Global Change—A Review. Remote Sensing, 15(7), Article 7. https://doi.org/10.3390/rs15071857

Rocha, N. S. da, Käfer, P. S., Skokovic, D., Veeck, G., Diaz, L. R., Kaiser, E. A., Carvalho, C. M., Cruz, R. C., Sobrino, J. A., Roberti, D. R., & Rolim, S. B. A. (2020). The Influence of Land Surface Temperature in Evapotranspiration Estimated by the S-SEBI Model. Atmosphere, 11(10), Article 10. https://doi.org/10.3390/atmos11101059

RTVSLO. (2022, 6). Kras je najzahtevnejše področje za obnovo gozda. Sadi in seje se praktično v kamen. https://www.rtvslo.si/okolje/kras-je-najzahtevnejse-podrocje-za-obnovo-gozda-sadi-in-seje-se-prakticno-v-kamen/635476

Shiff, S., Helman, D., & Lensky, I. M. (2021). Worldwide continuous gap-filled MODIS land surface temperature dataset. Scientific Data, 8(1), 74. https://doi.org/10.1038/s41597-021-00861-7

STA. (2023). Mineva Leto Dni Od Požara Na Krasu. https://www.sta.si/v-srediscu/pozar-kras-obletnica

STAGE. (2024). https://gis.stat.si/

Sun, X., Tang, H., Yang, P., Hu, G., Liu, Z., & Wu, J. (2020). Spatiotemporal patterns and drivers of ecosystem service supply and demand across the conterminous United States: A multiscale analysis. Science of The Total Environment, 703, 135005. https://doi.org/10.1016/j.scitotenv.2019.135005

SURS. (2023, 5). https://www.stat.si/StatWeb/News/Index/11124

TerrSet. (2020). Geospatial Monitoring and Modeling Software. https://clarklabs.org/terrset/

Tomlinson, C. J., Chapman, L., Thornes, J. E., & Baker, C. (2011). Remote sensing land surface temperature for meteorology and climatology: A review. Meteorological Applications, 18(3), 296–306. https://doi.org/10.1002/met.287

Ullah, W., Ahmad, K., Ullah, S., Tahir, A. A., Javed, M. F., Nazir, A., Abbasi, A. M., Aziz, M., & Mohamed, A. (2023). Analysis of the relationship among land surface temperature (LST), land use land cover (LULC), and normalized difference vegetation index (NDVI) with topographic elements in the lower Himalayan region. Heliyon, 9(2), e13322. https://doi.org/10.1016/j.heliyon.2023.e13322

UNICEF. (2023). Protecting Children from Heat Stress: A technical note (p. 54). https://www.unicef.org/media/139926/file/Protecting-children-from-heat-stress-A-technical-note-2023.pdf

Ünsal, Ö., Lotfata, A., & Avcı, S. (2023). Exploring the Relationships between Land Surface Temperature and Its Influencing Determinants Using Local Spatial Modeling. Sustainability, 15(15), Article 15. https://doi.org/10.3390/su151511594

USGS. (2024). EarthExplorer. https://earthexplorer.usgs.gov/

Vargas Zeppetello, L. R., Raftery, A. E., & Battisti, D. S. (2022). Probabilistic projections of increased heat stress driven by climate change. Communications Earth & Environment, 3(1), Article 1. https://doi.org/10.1038/s43247-022-00524-4

Veble, D., & Brečko Grubar, V. (2016). Pogostost in obseg požarov v naravi na Krasu in v slovenski Istri. Geografski Vestnik, 88(1), 9–20.

WMO. (2023, June 20). Climate Change Impacts Scar Europe, but Increase in Renewables Signals Hope for Future. https://wmo.int/news/media-centre/climate-change-impacts-scar-europe-increase-renewables-signals-hope-future

Zakšek, K., Marsetič, A., & Kokalj, Ž. (2007). Izkoriščanje sončne energije na Krasu. Geodetski Vestnik, 51(1), 35–47.

Zhang, Z., Li, J., Fung, T., Yu, H., Mei, C., Leung, Y., & Zhou, Y. (2021). Multiscale geographically and temporally weighted regression with a unilateral temporal weighting scheme and its application in the analysis of spatiotemporal characteristics of house prices in Beijing. International Journal of Geographical Information Science. https://www.tandfonline.com/doi/abs/10.1080/13658816.2021.1912348

Zhou, J., Teuling, A. J., Seneviratne, S., & Hirsch, A. (2022). Increasing population exposure to future heatwaves influenced by land-atmosphere interactions. https://doi.org/10.21203/rs.3.rs-1990379/v1

Žiberna, I., Pipenbaher, N., Donša, D., Škornik, S., Kaligarič, M., Bogataj, L. K., Črepinšek, Z., Grujić, V. J., & Ivajnšič, D. (2021). The Impact of Climate Change on Urban Thermal Environment Dynamics. Atmosphere, 12(9), Article 9. https://doi.org/10.3390/atmos12091159

Povzetek

Temperatura površja (ang. *Land surface temperature, LST*) je ključna spremenljivka za monitoring okoljskih sprememb in njihovih vplivov na podnebje in biosfero. V raziskavi na Natura 2000 območju Kras smo uporabili satelitske posnetke in podnebne projekcije, ki smo jih obdelali z metodo geografsko obtežene regresije (ang. *Multiscale geographically weighted regression, MGWR*). Glavni rezultat je napovedni model, ki na podlagi temperature zraka (ang. *mean daily air temperature, TAS*) in vegetacijskega indeksa (ang. *normalized difference vegetation index, NDVI*) kaže prihodnje vrednosti LST v primeru optimističnih in pesimističnih scenarijev skupnega družbeno-ekonomskega razvoja (ang. *Shared Socioeconomic Pathways, SSP*). Praktično smo na ta način prostorsko izboljšali spremenljivko TAS in tako ocenili potencialen vpliv toplotnega stresa na prebivalstvo na obravnavanem območju.

Rezultati kažejo večjo prostorsko variabilnost sedanjih vrednosti LST, ki segajo od 19,27 °C do 29,72 °C. Kot pričakovano so višje vrednosti LST značilne za pozidana in nižje ležeča območja, medtem ko so nižje vrednosti značilne za gozdnata in višjih ležeča območja. Natančneje, višje vrednosti LST so koncentrirane v osrednjem delu okoli Komna ter severozahodnem in južnem delu raziskovalnega območja, medtem ko so nižje vrednosti značilne za obrobje Krasa.

Predvideno je, da bodo prihodnje podnebne razmere povzročile povišanje temperature zraka, tako da so v skoraj vseh napovednih obdobjih pričakovana povišanja vrednosti LST (in posledično TAS). Kljub blažilnemu vplivu vegetacije, ki se bo po pričakovanjih širila zaradi pogozdovanja in ogozdovanja, splošni trend kaže na višje vrednosti LST in povečan toplotni stres. Obsežnejše in močnejše segrevanje je predvideno predvsem v južnih in osrednjih delih Krasa, zlasti na pozidanih in manj poraslih območjih.

Napovedni model kaže, da se bo izpostavljenost toplotnemu stresu močno povečala, kar bo lahko prizadelo predvsem mlado in starejše prebivalstvo. Glede na demografsko staranje Slovenije se bo občutljivost na toplotni stres še krepila. Poleg toplotnega stresa prebivalstva lahko povišane temperature tal in zraka vplivajo na biodiverziteto, tradicionalne dejavnosti, kot je proizvodnja kraškega pršuta, širjenje prenosljivih bolezni, požare, sušo, dostopnost vode, turizem in onesnaževanje.

Uporaba MGWR v raziskavi je omogočila novo razumevanje vzorcev toplotnega stresa na Natura 2000 območju Kras v različnih scenarijih podnebnih sprememb. Naše ugotovitve kažejo velike razlike med optimističnimi in pesimističnimi scenariji, kar nakazuje na velike potencialne koristi izvajanja učinkovitih podnebnih politik. Sonaravni ukrepi imajo lahko ključno vlogo pri zmanjševanju toplotnega stresa, ohranjanju biodiverzitete, izboljšanju zdravja, povečanju prehranske varnosti, zagotavljanju delovnih mest in povečanju sekvestracije ogljika. Raziskava poudarja tudi izzive, ki jih prinašajo demografske spremembe, predvsem naraščanje deleža starejših. Zaradi nevarnih posledic podnebnih sprememb za ranljivo prebivalstvo so potrebni ciljno usmerjeni ukrepi javnega zdravja in urbanističnega načrtovanja. Tako se lahko s celovitimi in proaktivnimi strategijami zagotovi odpornost ekosistemov in kakovost bivalnega okolja družbo.